Stability Analysis of Hybrid Integrator-Gain Systems: A Frequency-Domain Approach

S.J.A.M. van den Eijnden, M.F. Heertjes, H. Nijmeijer, W.P.M.H. Heemels

Eindhoven University of Technology, Department of Mechanical Engineering, 5600 MB Eindhoven, The Netherlands

Abstract

The hybrid integrator-gain system (HIGS) has been introduced recently with the aim to overcome fundamental limitations of linear time-invariant (LTI) control systems. To support the analysis and design of HIGS-based controllers, in this paper a novel frequency-domain condition for stability analysis of the feedback interconnection of an LTI system and HIGS is presented. Compared to existing frequency-domain stability conditions such as the one extending the circle-criterion, the condition presented in this paper exploits explicit knowledge regarding HIGS' switching strategy, thereby potentially providing a significantly less conservative condition. In particular, the novel condition in this paper guarantees the existence of a quadratic Lyapunov function that does not need to be positive definite within the full state space. The proposed condition can be verified graphically in a manner that is reminiscent of the classical Popov plot, as will be illustrated in an experimental case-study.

Key words: HIGS; stability analysis, frequency-domain; KYP-lemma

1 Introduction

The development of nonlinear control strategies that can overcome fundamental limitations of linear time-invariant (LTI) control for LTI systems [1] has a long history starting with the introduction of the Clegg integrator [2]. Since then, many alternative strategies have been proposed, including generalized reset elements [3], [4], [5], [16], [6], split-path nonlinear filters [7], [8], and hybrid integrator-gain systems (HIGS) [9], [10]. HIGS recently gained a lot of attention due to its ability to overcome well-known fundamental limitations of LTI control [10], next to its successful use in several engineering applications [12], [13]. These promising results indicate the potential of HIGS-based control, but to enable its wide dissemination it is important to build a strong analysis and design toolbox. While linear systems lend themselves well for robust stability and performance analysis through frequency-domain tools such as Nyquist and Bode plots [31], the switching nature of a control system with HIGS obstructs direct use of such tools. As the current industrial control practice highly exploits frequency-domain tools, it is important to develop similar tools for hybrid control strategies such as HIGS as well to support their wide adoption in practice.

The above need spurred the development of frequency-domain tools for stability analysis of switched and hybrid systems, see, *e.g.*, [19], [20], [22], [21], [23], [24], [16], [9], [17], [18], [25]. Underlying these tools is the well-known Kalman-Yakubovich-Popov (KYP) lemma [27], which allows for establishing the equivalence between frequency-domain conditions and the existence of a Lyapunov function. In principle, the frequency-domain conditions can be verified using *measured* frequency-response function (FRF) data of the plant to be controlled, thereby making them useful in practical situations, where sufficiently accurate state space models of the plant are often difficult, if not impossible, to obtain. Moreover, such frequency-domain conditions can be extended towards *robust* stability analysis.

Although valuable from a practical perspective, existing frequency-domain conditions that are applicable to the class of HIGS-based control systems, such as the ones presented in, *e.g.*, [9],[19], often provide a rather conservative estimate on the region of closed-loop stability.

To some extent, this conservatism is caused by the fact that the conditions do not sufficiently take into account the particular switching characteristics of HIGS, and by regarding HIGS as a generic sector-bounded nonlinearity its underlying dynamics are ignored [9]. It is interesting to remark that in all aforementioned works, the Lyapunov function that results from satisfying the conditions is guaranteed to be positive *within the full state space*. This may be a restrictive feature of these results, because HIGS is sector-bounded, and thus trajectories of a closed-loop system with HIGS are confined to a subset of the state space.

The main contribution of this paper is the development of novel frequency-domain conditions for stability analysis of the feedback interconnection of an LTI system and HIGS. These conditions are novel in the sense that, if satisfied, they guarantee the existence of a quadratic Lyapunov function that is not necessarily positive definite within the full state space, but rather in a subset of the state space where HIGS operates. The same holds true for negative definiteness of its corresponding time-derivative. To the best of the authors' knowledge, frequency-domain conditions for guaranteeing the existence of a Lyapunov function that does not need to be positive definite within the full state space have not been established in the literature before. The new frequency-domain conditions are a generalization of our preliminary results in the conference paper [28], and can be verified graphically in a manner that is comparable with the classical Popov plot [15]. We will demonstrate by means of a practical example that our new frequency-domain condition can show stability in relevant situations where existing results can not be applied.

The remainder of this paper is organized as follows. Some preliminary results are introduced in Section 2. The system setting and the problem formulation are discussed in Section 3. In Section 4, the main results of this paper are presented in the form of a theorem that sets forth graphically verifiable frequency-domain stability conditions. Application of the presented results is demonstrated on an experimental motion set-up in Section 5. A summary of the main conclusions is provided in Section 6.

2 Preliminaries

2.1 Notation and definitions

The following notations and definitions are used. A single-input single-output (SISO) transfer function $G(s)$, $s \in \mathbb{C}$, with real coefficients, is said to be stable, if all its poles are located in the open left-half complex plane. The real and imaginary parts of a (complex) frequency response function $G(j\omega) \in \mathbb{C}$, $\omega \in \mathbb{R}$, are denoted by $\text{Re}\{G(j\omega)\}$ and $\text{Im}\{G(j\omega)\}$, respectively, and the complex conjugate is indicated by $G^*(j\omega)$, which

is equal to $G(-j\omega)$. The set of real symmetric matrices in $\mathbb{R}^{n \times n}$ is denoted by $\mathbb{S}^{n \times n}$. A symmetric matrix $M \in \mathbb{S}^{n \times n}$ is positive (semi-)definite, denoted by $M \succ 0$ ($M \succeq 0$), if $x^\top M x > 0$ for all $x \in \mathbb{R}^n \setminus \{0\}$ ($x^\top M x \geq 0$ for all $x \in \mathbb{R}^n$). Negative (semi-)definite matrices are denoted in a similar manner by reversing the inequalities. A matrix $A \in \mathbb{R}^{n \times n}$ is said to be Hurwitz, if all its eigenvalues have strictly negative real part. For matrices we use the shorthand notations $\text{He}(X) = X + X^\top$ and $\text{Pr}(X) = X^\top X$. The inequality symbols $>, \geq, <, \leq$ for vectors are understood componentwise.

2.2 Fundamental result

A general version of the well-known KYP-lemma, which is free of any hypothesis on minimality of the system, is provided. This fundamental result plays a central role in the proof of the paper's main theorem.

Theorem 1 ([27, Theorem 1]) *Given* $A \in \mathbb{R}^{n \times n}$, $B \in \mathbb{R}^{n \times m}$, $Q \in \mathbb{S}^{(n+m) \times (n+m)}$ *with* $\det(j\omega I - A) \neq 0$ *for all* $\omega \in \mathbb{R}$. *The next two statements are equivalent:*

(1) The following inequality holds for all $\omega \in \mathbb{R} \cup \{\infty\}$

$$\begin{bmatrix} (j\omega I - A)^{-1}B \\ I \end{bmatrix}^* Q \begin{bmatrix} (j\omega I - A)^{-1}B \\ I \end{bmatrix} \prec 0. \quad (1)$$

(2) There exists a matrix $P \in \mathbb{S}^{n \times n}$ *such that*

$$\begin{bmatrix} A^\top P + PA & PB \\ B^\top P & 0 \end{bmatrix} + Q \prec 0. \quad (2)$$

The equivalence holds for non-strict inequalities in both (1) *and* (2), *if the pair* (A, B) *is controllable.*

3 System setting and problem formulation

3.1 Closed-loop system description

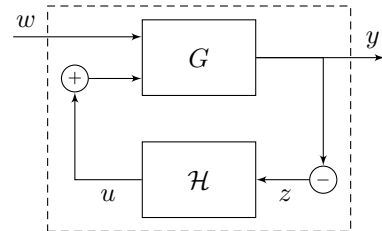Throughout this paper, we consider the generic closed-loop system setting as depicted in Fig. 1.

Fig. 1. Interconnection of an LTI system G and HIGS $\mathcal{H}$.

In Fig. 1, the LTI system G (containing the plant to be controlled, along with possible LTI controller elements) is given by

$$G : \begin{cases} \dot{x}_g & = A_g x_g + B_g u + B_w w, \\ y & = C_g x_g, \end{cases} \tag{3}$$

with states $x_g \in \mathbb{R}^m$, exogenous inputs $w \in \mathbb{R}^v$, control input $u \in \mathbb{R}$, and output $y \in \mathbb{R}$. We assume that (A_g, B_g, C_g) is minimal and the transfer functions from u to y and w to y are denoted by

$$\left[G_{yu}(s) \ G_{yw}(s) \right] = C_g(sI - A_g)^{-1} \left[B_g \ B_w \right]. \tag{4}$$

For many physical systems, such as motion systems containing floating masses, the next assumption on the relative degree of the system is generally satisfied.

Assumption 2 *The transfer functions $G_{yu}(s)$ and $G_{yw}(s)$ given in (4) have a relative degree of at least two, such that $C_g B_g = C_g B_w = 0$.*

The hybrid integrator-gain system $\mathcal{H}$ is described by

$$\mathcal{H} : \begin{cases} \dot{x}_h & = \omega_h z, \text{ if } (z, u, \dot{z}) \in \mathcal{F}_1, \\ x_h & = k_h z, \text{ if } (z, u, \dot{z}) \in \mathcal{F}_2, \\ u & = x_h, \end{cases} \tag{5}$$

where $x_h \in \mathbb{R}$ denotes the integrator state, $z = -y \in \mathbb{R}$ is the input to HIGS, and $u \in \mathbb{R}$ is the generated output. Within the context of Fig. 1 and under Assumption 2, z is continuously differentiable, and $\dot{z} = -\dot{y} = -C_g A_g x_g$ denotes the corresponding time-derivative. The parameters $\omega_h \in (0, \infty)$ and $k_h \in (0, \infty)$ in (5) are the integrator frequency and gain, respectively. The sets $\mathcal{F}_1$ and $\mathcal{F}_2$ dictating the integrator-mode and gain-mode in (5) are given by

$$\mathcal{F}_1 = \left\{ (z, u, \dot{z}) \in \mathbb{R}^3 \mid k_h z u \geq u^2 \wedge (z, u, \dot{z}) \notin \mathcal{F}_2 \right\}, \tag{6a}$$

$$\mathcal{F}_2 = \left\{ (z, u, \dot{z}) \in \mathbb{R}^3 \mid u = k_h z \wedge \omega_h z^2 > k_h \dot{z} z \right\}, \tag{6b}$$

for which the union defines the "$[0, k_h]$-sector"

$$\mathcal{F} := \mathcal{F}_1 \cup \mathcal{F}_2 = \left\{ (z, u, \dot{z}) \in \mathbb{R}^3 \mid k_h z u \geq u^2 \right\}. \tag{7}$$

The closed-loop system in Fig. 1 with G as in (3), and $\mathcal{H}$ as in (5), (6) can be written as the switched system

$$\begin{aligned} \dot{x} &= A_i x + B w, \text{ if } x \in \mathcal{X}_i, \, i \in \{1, 2\}, \\ y &= C x, \end{aligned} \tag{8}$$

with state vector $x = [x_g^\top, x_h]^\top \in \mathbb{R}^n$, $n = m + 1$. The sets $\mathcal{X}_i$, $i \in \{1, 2\}$, in (8) are given by

$$\mathcal{X}_i = \left\{ x \in \mathbb{R}^n \mid Ex \in \mathcal{F}_i \right\}, \tag{9}$$

in which the matrix E is such that $Ex = [z \, u \, \dot{z}]^\top$, and is, therefore, given by

$$E^\top = \begin{bmatrix} -C_g^\top & 0 & -(C_g A_g)^\top \\ 0 & 1 & 0 \end{bmatrix}. \tag{10}$$

The mode-dependent system matrices are given by

$$A_1 = \begin{bmatrix} A_g & B_g \\ -\omega_h C_g & 0 \end{bmatrix}, \quad A_2 = \begin{bmatrix} A_g & B_g \\ -k_h C_g A_g & 0 \end{bmatrix}, \tag{11}$$

$B = [B_w^\top, \, 0]^\top$, and $C = [C_g, \, 0]$. Details on the sets in (6), as well as an alternative view on the closed-loop system (8) within the framework of (extended) projected dynamical systems (ePDS) can be found in [9], [26].

To show the existence and forward completeness of solutions to (8), we rely on the well-posedness result in [26, Theorem 8]. We consider solutions to the discontinuous differential equation (8) in the sense of Carathéodory, *i.e.*, locally absolutely continuous (AC) functions $x : [0, T] \to \mathbb{R}^n$ that satisfy (8) for almost all times $t \in [0, T]$. The results in [26] guarantee the existence of solutions globally, *i.e.*, on $[0, \infty)$, given an initial condition $x(0) = x_0$ and a bounded piecewise continuous input w, *i.e.*, $w \in \mathbb{PC}$, meaning that there is $\{t_k\}_{k \in \mathbb{N}} \subset [0, \infty)$ with $t_0 = 0$, $t_{k+1} > t_k$ for all $k \in \mathbb{N}$, $\lim_{k \to \infty} t_k = \infty$, w is continuous for all $t \notin \{t_k\}_{k \in \mathbb{N}}$, and $\lim_{t \downarrow t_k} w(t) = w(t_k)$, $k \in \mathbb{N}$, and $\|w\|_\infty = \sup_t \|w(t)\| < \infty$.

3.2 Problem formulation

We are concerned with deriving *sufficient* frequency-domain-based conditions for assessing stability of the closed-loop system in (8). Stability is studied through the notion of *input-to-state stability* (ISS), for which the following definition [1] is adopted from [11].

Definition 3 *The closed-loop system in (8) is said to be input-to-state stable (ISS), if there exist a $\mathcal{KL}$-function α and a $\mathcal{K}$-function β such that for any initial condition $x(0) = x_0 \in \{x \in \mathbb{R}^n \mid Ex \in \mathcal{F}\}$ and any input signal $w \in \mathbb{PC}$, all solutions $x : \mathbb{R}_{\geq 0} \to \mathbb{R}^n$ to (8) satisfy*

$$\|x(t)\| \leq \alpha(\|x(0)\|, t) + \beta(\|w\|_\infty), \tag{12}$$

for all $t \in \mathbb{R}_{\geq 0}$.

The next theorem presents LMI-based conditions for guaranteeing ISS of the closed-loop system (8).

---

[1] In Definition 3 we adopt standard definitions for class $\mathcal{K}$- and class $\mathcal{KL}$-functions, see, *e.g.*, [15, Ch. 40, Sec. 4.4].

Theorem 4 ([29, Theorem 1]) *Consider the closed-loop system* (8). *Suppose there exist a matrix $P \in \mathbb{S}^{n \times n}$ and constants $\tau_i \geq 0$, $i \in \{1, 2, 3\}$, that satisfy the LMIs*

$$P - \tau_1 S \succ 0, \qquad (13a)$$

$$A_1^\top P + P A_1 + \tau_2 S \prec 0, \qquad (13b)$$

$$\Theta^\top (A_2^\top P + P A_2 - \tau_3 T) \Theta \prec 0, \qquad (13c)$$

in which

$$S = C_u^\top H + H^\top C_u, \quad T = C_u^\top F + F^\top C_u, \qquad (14)$$

and $\Theta = [I, -k_h C_g^\top]^\top$, with $H = k_h C_z - C_u$, $F = C_z(k_h A_1 - \omega_h I)$, and where

$$C_z = \begin{bmatrix} -C_g & 0 \end{bmatrix}, \text{ and } C_u = b^\top = \begin{bmatrix} 0_m & 1 \end{bmatrix}. \qquad (15)$$

Then, the closed-loop system (8) *is ISS.*

Although numerically tractable, solving the LMIs in (13) requires a state-space model as in (3), which, in practice, may be hard to obtain with sufficient accuracy. Moreover, LMI conditions provide limited insights in the (re)design of HIGS-based controllers for guaranteed (robust) stability when the set of LMIs (13) turns out to be infeasible. Motivated by these concerns, the main objective in this paper is to establish insightful *frequency-domain* conditions that exploit frequency-response data of the plant for guaranteeing ISS. In particular, we are interested in deriving sufficient frequency-domain conditions that guarantee the existence of a matrix P and constants τ_i, $i \in \{1, 2, 3\}$, that satisfy the inequalities in (13), thereby transitioning from time-domain conditions to frequency-domain conditions for guaranteeing ISS.

4 Frequency-domain conditions for ISS

4.1 Existing results

Frequency-domain conditions for guaranteeing ISS of HIGS-controlled systems have been established in the literature before. Although useful, these conditions come with a certain degree of conservatism in the sense that they guarantee the existence of a *particular* solution to the LMI problem in (13). To shed some light on this possible conservatism, and motivate our new improved conditions, we recall these existing results.

Theorem 5 ([9, Theorem 6.1]) *Suppose the matrix A_g in (3) is Hurwitz. If the frequency-domain inequality*

$$\mathrm{Re}\left\{ k_h C_g (j\omega I - A_g)^{-1} B_g \right\} > -1 \qquad (16)$$

is satisfied for all $\omega \in \mathbb{R} \cup \{\infty\}$, then the LMI problem in (13) admits a feasible solution of the form $P = \mathrm{diag}(M, 1) \succ 0$, with positive definite matrix $M \in \mathbb{S}^{m \times m}$, $\tau_1 = 0$, and $\tau_2, \tau_3 \geq 0$.

Theorem 6 ([28, Theorem 1]) *Suppose the matrix A_1 in (11) is Hurwitz. If there exist constants $\alpha_1 \geq 0$ and $\alpha_2 \in \mathbb{R}$ such that the frequency-domain inequality*

$$\mathrm{Re}\left\{ (F + \alpha_1 C_z + \alpha_2 H)(j\omega I - A_1)^{-1} b \right\} > -1 \qquad (17)$$

is satisfied for all $\omega \in \mathbb{R} \cup \{\infty\}$, then the LMI problem in (13) admits a feasible solution of the form $P \succ 0$, $\tau_1 = \tau_2 = 0$, and $\tau_3 \geq 0$.

The link between satisfying the frequency-domain inequalities in Theorem 5 and 6, and the existence of a particular solution to the LMI problem in Theorem 4, allows for establishing the following important insights regarding possible conservatism of these conditions:

(1) As a consequence of the fact that both theorems guarantee the existence of a solution to the LMI problem (13) with $\tau_1 = 0$, an ISS-Lyapunov function $V(x) = x^\top P x$ is guaranteed to be positive for all $x \in \mathbb{R}^n \setminus \{0\}$, while the states of the closed-loop system (8) only evolve, by design, in part of the state space. This observation reveals possible conservatism induced by the considered class of Lyapunov functions underlying Theorem 5 and 6.

(2) Theorem 5 is applicable to HIGS-based control systems for which G_{yu} is stable. However, in many applications that may benefit from HIGS-based control, such as motion systems, the linear part of the dynamics contains simple integrators, which renders the circle-criterion-like conditions in Theorem 5 not straightforwardly applicable as G_{yu} is not stable. For condition (16) also the interplay between the LTI dynamics and the integrator-dynamics of HIGS is not exploited, and stability holds for all (static) sector-bounded nonlinearities. This is also visible from the fact that the frequency-domain inequality in (16) does not depend on the integrator parameter ω_h.

(3) Theorem 6 is only applicable to HIGS-based control systems having stable linear dynamics in integrator-mode. This narrows down the scope of applications for which Theorem 6 may be useful for stability analysis. In fact, one may argue that unstable integrator-mode dynamics largely contribute to potential performance improvements with HIGS, and, therefore, is a desirable property (see, for instance, [9], [10]).

In conclusion, although the results in Theorem 5 and Theorem 6 are of interest, they suffer from restrictions that are not always beneficial for HIGS-based designs. Therefore, obtaining frequency-domain conditions in which the above limitations are lifted is considered important for useful practical application.

4.2 Main result

To address the previously discussed shortcomings and provide less restrictive conditions, we present the next theorem, which forms the main result of this paper.

Theorem 7 *Suppose the matrix $A_g - k_h B_g C_g$ is Hurwitz. If there exist constants $\lambda \geq 0$ and $k \geq 1$ such that the frequency-domain inequality*

$$\text{Re}\left\{ (F + \beta_1 C_u + \beta_2 H)\, (j\omega I - \mathcal{A}_2)^{-1}\, b \right\} > -1 \quad (18)$$

with $\mathcal{A}_2 = A_2 + k\frac{\omega_h}{k_h} bH$ and $\beta_1 = \lambda k$, $\beta_2 = \lambda + k\frac{\omega_h}{k_h}$ is satisfied for all $\omega \in \mathbb{R} \cup \{\infty\}$, then the LMI problem in (13) admits a feasible solution of the form

$$P = M + \lambda H^\top H + \tau_1 S \quad (19)$$

with $M \succ 0$, and S given in (14), $\tau_1 = \lambda k \geq 0$, $\tau_2 = \tau_1(k-1)\frac{\omega_h}{k_h} \geq 0$, and $\tau_3 = 0$.

The main advantages of Theorem 7 as compared to Theorem 5 and Theorem 6 are as follows. First, the frequency-domain condition (18) guarantees the existence of a feasible solution to the LMIs in (13) with $\tau_1 \geq 0$, such that an ISS-Lyapunov function constructed as $V(x) = x^\top P x$ with P in (19) is guaranteed to be positive for all $x \in \mathcal{X}_1 \cup \mathcal{X}_2$, with $\mathcal{X}_i$, $i = \{1, 2\}$ given in (9). Note here that P in (19) itself is not necessarily a positive definite matrix, as the matrix S given in (14) is indefinite. Second, the conditions allow for both unstable plant dynamics, as well as unstable integrator-mode dynamics, which, from a performance perspective can be desirable. We will explain below in Section 4.3 how the frequency-domain condition (18) can be checked in a manner that is reminiscent of the classical Popov test.

PROOF. By the assumption that the matrix $A_g - k_h B_g C_g$ is Hurwitz and $k \geq 1$, the matrix

$$\mathcal{A}_2 = A_2 + k\frac{\omega_h}{k_h} bH$$

$$= \begin{bmatrix} A_g & B_g \\ -k_h C_g A_g & 0 \end{bmatrix} + k\frac{\omega_h}{k_h} \begin{bmatrix} 0_m \\ 1 \end{bmatrix} \begin{bmatrix} -k_h C_g & -1 \end{bmatrix} \quad (20)$$

is Hurwitz as well. To see this, consider the similarity transformation $\mathcal{T}\mathcal{A}_2\mathcal{T}^{-1}$ with transformation matrices

$$\mathcal{T} = \begin{bmatrix} I & 0 \\ k_h C_g & 1 \end{bmatrix}, \quad \text{and} \quad \mathcal{T}^{-1} = \begin{bmatrix} I & 0 \\ -k_h C_g & 1 \end{bmatrix}, \quad (21)$$

leading to

$$\bar{\mathcal{A}}_2 := \mathcal{T}\mathcal{A}_2\mathcal{T}^{-1} = \begin{bmatrix} A_g - k_h B_g C_g & B_g \\ 0 & -k\frac{\omega_h}{k_h} \end{bmatrix}. \quad (22)$$

Due to its upper triangular structure, the eigenvalues of the transformed matrix $\bar{\mathcal{A}}_2$ in (22) are given by the eigenvalues of $A_g - k_h B_g C_g$ and $-k\omega_h/k_h$. Therefore, $\bar{\mathcal{A}}_2$ is Hurwitz, and thus $\mathcal{A}_2$ is Hurwitz as well.

Next, note that the frequency-domain inequality (18) can be written in the form of (1) with Q given by

$$Q = \begin{bmatrix} 0 & -(F + \beta_1 C_u + \beta_2 H)^\top \\ \star & -2 \end{bmatrix}. \quad (23)$$

Under the assumption that (18) is satisfied for all $\omega \in \mathbb{R} \cup \{\infty\}$, and since $\mathcal{A}_2$ is Hurwitz, it follows by virtue of the KYP-lemma (Theorem 1) that there exists a matrix $M = M^\top \in \mathbb{S}^{n \times n}$ such that

$$\begin{bmatrix} \mathcal{A}_2^\top M + M\mathcal{A}_2 & Mb - (F + \beta_1 C_u + \beta_2 H)^\top \\ \star & -2 \end{bmatrix} \prec 0. \quad (24)$$

Define

$$Mb - (F + \beta_1 C_u + \beta_2 H)^\top = \sqrt{2} L^\top \quad (25)$$

and apply the Schur complement to (24) to find that this inequality is equivalent to

$$\mathcal{A}_2^\top M + M\mathcal{A}_2 \prec -L^\top L. \quad (26)$$

Clearly, as (26) implies $\mathcal{A}_2^\top M + M\mathcal{A}_2 \prec 0$, and $\mathcal{A}_2$ is Hurwitz, it follows immediately from, *e.g.*, [14, Lemma 1.10.1] that $M \succ 0$.

We will show that (25), (26) imply satisfaction of (13). To show (13a), let us construct a suitable matrix P as

$$P = M + \lambda H^\top H + \lambda k S. \quad (27)$$

It clearly follows that (13a) is satisfied with $\tau_1 = \lambda k$. Next, we will show that (13b) is satisfied. To do this, first we write $\mathcal{A}_2 = A_1 + bG$ with $G := F + k\frac{\omega_h}{k_h} H$, where F is given in (14). Using this identity in (26) implies

$$A_1^\top M + M A_1 \prec -G^\top b^\top M - MbG - L^\top L$$
$$\overset{(25)}{=} -\text{He}\left(\lambda(kC_u + H) + G - \sqrt{2}L \right)^\top G - L^\top L$$
$$= -\text{Pr}\left(L - \sqrt{2}G \right) - \text{He}\left(\lambda(kC_u + H)^\top G \right) \quad (28)$$
$$\preceq -\lambda \text{He}\left((kC_u + H)^\top \left(F + k\frac{\omega_h}{k_h} H \right) \right).$$

Observe that by virtue of Assumption 2 we can write

$$F = C_z(k_h A_1 - \omega_h I) = \begin{bmatrix} -C_g & 0 \end{bmatrix} \begin{bmatrix} k_h A_g - \omega_h I & k_h B_g \\ -k_h \omega_h C_g & -\omega_h \end{bmatrix}$$

$$= \begin{bmatrix} -k_h C_g A_g - \omega_h C_g & 0 \end{bmatrix} = H A_1,$$

recalling that $H = [-k_h C_g, \; -1]$. As such,

$$\begin{aligned}
(kC_u + H)^\top F &= (kC_u + H)^\top H A_1 \\
&= (kS + H^\top H - kH^\top C_u)A_1 \qquad (29) \\
&= (kS + H^\top H)A_1 - k\omega_h H^\top C_z,
\end{aligned}$$

where use is made of the identities $S = C_u^\top H + H^\top C_u$ and $C_u A_1 = \omega_h C_z$. Substituting (29) in (28) yields

$$\begin{aligned}
&\mathrm{He}\big((M + \lambda H^\top H + \lambda k S)A_1\big) \\
&+ \lambda k \frac{\omega_h}{k_h}\mathrm{He}\Big(\big(kC_u + H - k_h C_z\big)^\top H\Big) \prec 0.
\end{aligned} \qquad (30)$$

The last term in the left-hand side of (30) reads

$$(kC_u + H - k_h C_z)^\top H = (k-1)C_u^\top H.$$

Under the assumption that $k \geq 1$, using again the identity $S = C_u^\top H + H^\top C_u$ and using P as constructed in (27) this yields

$$A_1^\top P + P A_1 + \tau_2 S \prec 0 \qquad (31)$$

with $\tau_2 = \lambda k(k-1)\omega_h/k_h \geq 0$. Thus, (13b) is satisfied.

It remains to show that (13c) is satisfied. To this end, note that from the inequality in (26) and the construction of P in (27) we find that

$$\begin{aligned}
0 &\succ \mathcal{A}_2^\top M + M\mathcal{A}_2 = \mathrm{He}\big((P - \lambda H^\top H - \lambda k S)\mathcal{A}_2\big) \\
&= \mathrm{He}\big(P\mathcal{A}_2 - \lambda(H^\top H + kH^\top C_u + kC_u^\top H)\mathcal{A}_2\big) \\
&= \mathrm{He}\Big(P\mathcal{A}_2 - \lambda H^\top((H + kC_u)\mathcal{A}_2 + k^2 \frac{\omega_h}{k_h}C_u)\Big) \\
&= A_2^\top P + P\mathcal{A}_2 + (H^\top \Gamma^\top + \Gamma H)
\end{aligned}$$

with $\Gamma = k\frac{\omega_h}{k_h}(Pb + \lambda k C_u^\top) - \lambda \mathcal{A}_2^\top(H + kC_u)^\top$. Here, we used that $H\mathcal{A}_2 = 0$ and

$$C_u^\top H \mathcal{A}_2 = C_u^\top H\Big(A_2 + k\frac{\omega_h}{k_h}bH\Big) = -k\frac{\omega_h}{k_h}C_u^\top H. \qquad (32)$$

Since $H\Theta = 0$, we find $\Theta^\top(A_2 P + P\mathcal{A}_2)\Theta \prec 0$ and (13c) is satisfied with $\tau_3 = 0$. This completes the proof. $\qquad \square$

4.3 Verifying the frequency-domain conditions

At this point in the analysis it is not immediately clear how to verify the frequency-domain condition (18) in an effective manner. This is because (18) is still expressed in terms of state space matrices that may be difficult to obtain in practice, and the variables λ, k appear in (18) in a nonlinear manner. In order to derive an effective method for verifying the conditions using (measured) FRF data, we will first derive the relevant transfer function to be checked. Based on the frequency-domain condition in (18), this transfer function can be identified as

$$\mathcal{G}(s) := \mathcal{C}(sI - \mathcal{A}_2)^{-1}\mathcal{B} + \mathcal{D}, \qquad (33)$$

where $\mathcal{C} := F + \beta_1 C_u + \beta_2 H$, $\mathcal{B} := b$, and $\mathcal{D} := 1$. To rewrite (33) into known transfer functions, it is useful to first do a similarity transformation using the same transformation matrix $\mathcal{T}$ as in (21). Through standard manipulations this results in the equivalent transfer function

$$\mathcal{G}(s) = \hat{\mathcal{C}}(sI - \hat{\mathcal{A}}_2)^{-1}\hat{\mathcal{B}} + \hat{\mathcal{D}}, \qquad (34)$$

where

$$\left[\begin{array}{c|c} \hat{\mathcal{A}}_2 & \hat{\mathcal{B}} \\ \hline \hat{\mathcal{C}} & \hat{\mathcal{D}} \end{array}\right] = \left[\begin{array}{c|c} \mathcal{T}\mathcal{A}_2\mathcal{T}^{-1} & \mathcal{T}\mathcal{B} \\ \hline \mathcal{C}\mathcal{T}^{-1} & \mathcal{D} \end{array}\right] = \left[\begin{array}{cc|c} A_l & B_g & 0 \\ 0 & -k\frac{\omega_h}{k_h} & 1 \\ \hline Z & K & 1 \end{array}\right],$$

with $A_l := A_g - k_h B_g C_g$, $Z := C_g((\omega_h - k_h\beta_1)I - k_h A_g)$ and $K := \beta_1 - \beta_2$. Note the upper-triangular structure of the matrix $\hat{\mathcal{A}}_2$ and thus also of $sI - \hat{\mathcal{A}}_2$. The inverse of $sI - \hat{\mathcal{A}}_2$ can be computed as

$$\begin{aligned}
&(sI - \hat{\mathcal{A}}_2)^{-1} = \\
&\begin{bmatrix} (sI - A_k)^{-1} & (sI - A_l)^{-1}B_g(s + k\frac{\omega_h}{k_h})^{-1} \\ 0 & (s + k\frac{\omega_h}{k_h})^{-1} \end{bmatrix}.
\end{aligned} \qquad (35)$$

Substituting (35) into (34) yields

$$\mathcal{G}(s) = \big(Z(sI - A_l)^{-1}B_g + K\big)\Big(s + k\frac{\omega_h}{k_h}\Big)^{-1} + 1. \quad (36)$$

By realizing that $C_g(sI - A_l)^{-1}B_g$ corresponds to the process sensitivity of the linear gain-mode of the HIGS-controlled system (i.e., replacing HIGS in Fig. 1 by k_h), we find the transfer function to be checked to be given by

$$\mathcal{G}(s) = (W(s)S_P(s) + K)L(s) + 1, \qquad (37)$$

with $W(s) = \omega_h - k_h\beta_1 - k_h s$, $S_P(s) = G_{yu}(s)(1 + k_h G_{yu}(s))^{-1}$ and $L(s) = (s + k\omega_h/k_h)^{-1}$.

With the transfer function $\mathcal{G}(s)$ written in terms of known transfer functions, we can now continue describing the procedure for verifying the conditions of Theorem 7. As a first check, we should verify if the gain-mode dynamics are ISS, i.e., we should check if the matrix $A_l = A_g - k_h B_g C_g$ is Hurwitz. This can be done by applying the Nyquist stability criterion [30, Section 6.3] to the open-loop characteristics $1 + k_h G_{yu}(s)$. Note that (part of) the characteristics of $G_{yu}(s)$ may be obtained from FRF measurements. For verifying condition (18),

it is useful to rewrite (37) as

$$\mathcal{G}(s) = G_x(s) - \lambda G_y(s) + 1, \qquad (38)$$

where

$$G_x(s) := \left(\left(\omega_h - k_h s \right) S_P(s) - k \frac{\omega_h}{k_h} \right) L(s), \qquad (39a)$$

$$G_y(s) := \left(k k_h S_P(s) + (1 - k) \right) L(s). \qquad (39b)$$

Verifying the inequality in (18) then amounts to finding parameters $\lambda \geq 0$, $k \geq 1$ such that for all $\omega \in \mathbb{R} \cup \{\infty\}$ the frequency-domain inequality

$$1 + \mathrm{Re} \left\{ G_x(j\omega) \right\} - \lambda \mathrm{Re} \left\{ G_y(j\omega) \right\} > 0 \qquad (40)$$

is satisfied. For a fixed value of $k \geq 1$, verifying (40) can be done graphically by plotting $\mathrm{Re} \{G_y\}$ against $\mathrm{Re} \{G_x\}$ in a two-dimensional plane and inspecting if the resulting curve lies to the right of a straight line that passes through the point $(-1, 0)$ with a slope of $1/\lambda$. This graphical test shows strong resemblance with the classical Popov plot [15]. The parameter k should be searched for in an iterative manner. Note that the effect of changing k on the $(\mathrm{Re} \{G_x\}, \mathrm{Re} \{G_y\})$-curve is directly visible, and thus such a search can be done efficiently.

5 Case-study on a motion system

In this section, we demonstrate the efectiveness of our presented tools on an experimental motion system. The set-up consists of two rotating masses connected by a thin, flexible shaft as shown in Fig. 4. The measured FRF of this system from actuator input (left-side) to load position (right-side) is shown in Fig. 3.
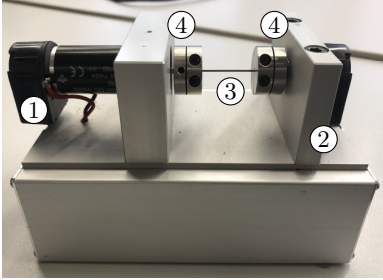
Fig. 2. Motor-load motion system. 1: actuator (motor side); 2: encoder (load side); 3: flexible shaft; 4: rotating masses.

5.1 Controller design

Consider the feedback control scheme as depicted in Fig. 4. Given a reference command $r : \mathbb{R}_{\geq 0} \to \mathbb{R}$, a servo error signal e is constructed using the relation $e(t) = r(t) - q(t)$, $t \in \mathbb{R}_{\geq 0}$, where $q(t) \in \mathbb{R}$ represents the measured output of the motor-load motion system P at time $t \in \mathbb{R}_{\geq 0}$. This system is subject to an input disturbance $d(t) \in \mathbb{R}$ for $t \in \mathbb{R}_{\geq 0}$. For dealing with distur-
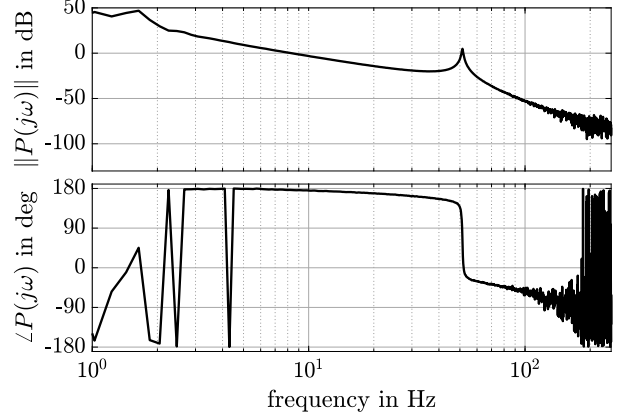
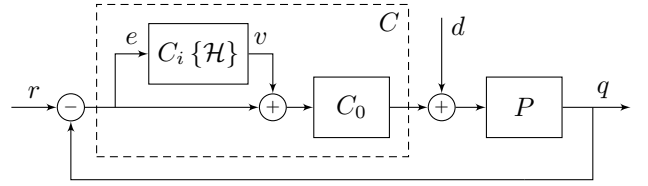Fig. 3. Measured FRF of the motor-load motion system.

Fig. 4. Feedback control set-up with controller C containing the HIGS-based integrator $C_i \{\mathcal{H}\}$.

bances, a feedback controller $C = (1 + C_i \{\mathcal{H}\})C_0$ with integral action is designed. The LTI filter C_0 is given by

$$C_0(s) = k_p \left(\frac{s + \omega_z}{s + \omega_p} \right) \left(\frac{\omega_{lp}^2}{s^2 + 2\beta_{lp}\omega_{lp}s + \omega_{lp}^2} \right), \quad (41)$$

whereas C_i is a HIGS-based integrator constructed as $C_i \{\mathcal{H}\} = L_1 \mathcal{H} L_2$, where

$$L_1(s) = \omega_i \left(\frac{s + \omega_c}{\tau s + 1} \right), \quad \text{and} \quad L_2(s) = \frac{\tau s + 1}{s}.$$

This specific design stems from describing function reasoning and is intended for balancing transient and steady-state performance properties by exploiting "phase" advantages of HIGS, see [10] for further details. Controller tuning is done by initially setting $\omega_h = \infty$ such that $C_i \{\mathcal{H}\}$ effectively reduces to an LTI integrator and the linear scheme $C(s) = (1 + \frac{\omega_i}{s})C_0(s)$ is recovered. Using classical loop-shaping techniques [31], a stable LTI design is obtained with $k_p = 3.3$ Nm, $\omega_i = 8 \cdot 2\pi$ rad/s, $\omega_z = 2 \cdot 2\pi$ rad/s, $\omega_p = \omega_{lp} = 50 \cdot 2\pi$ rad/s, and $\beta_{lp} = 0.5$. After fixing $k_h = 1$ Nm, and $\tau = 0.002$ s, ω_h is reduced to $\omega_h = 5 \cdot 2\pi$ rad/s.

To verify ISS of the closed-loop system design, we first write the configuration in Fig. 4 in terms of the Lur'e setting in Fig. 1. Specifically, we find the transfer func-
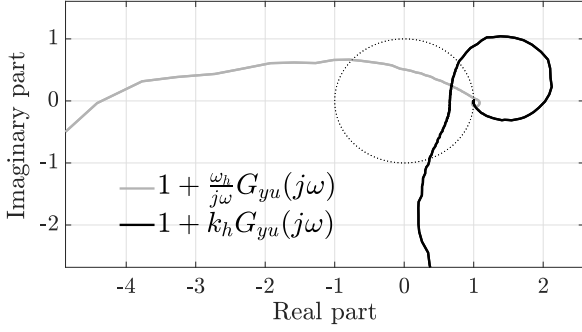
Fig. 5. Nyquist plot of the open-loop characteristics of the integrator-mode (grey) and gain-mode (black) using the measured FRF of the motor-load motion system.
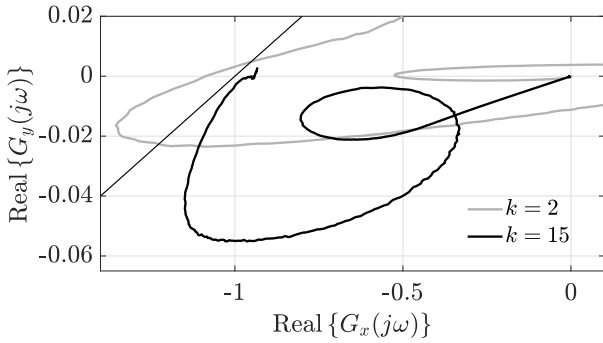

Fig. 6. Popov-like plot constructed on the basis of the measured FRF of the motor-load motion system and parameter values $k = \{2, 15\}$, $\lambda = 10$.

tion from output u to input $y = -z$ of $\mathcal{H}$ to be given by

$$G_{yu}(s) = L_1(s) \left(\frac{C_0(s)P(s)}{1 + C_0(s)P(s)} \right) L_2(s). \qquad (42)$$

Note that due to the simple integrator in $L_2(s)$, the linear portion of the closed-loop system is not asymptotically stable. Hence, for verifying ISS one cannot apply Theorem 5, but should resort to Theorem 6 or Theorem 7. In these theorems, we either need to verify stability of the integrator-mode (Theorem 6) or stability of the gain-mode (Theorem 7). This can be done by inspecting the Nyquist plots of the integrator-mode in open-loop, i.e., $1 + \frac{\omega_h}{s} G_{yu}(s)$ and the gain-mode in open-loop, i.e., $1 + k_h G_{yu}(s)$ which are both shown in Fig. 5.

On the basis of the Nyquist stability criterion, it follows from Fig. 5 that the integrator-mode is unstable, whereas the gain-mode is stable. Hence, one cannot apply Theorem 6 either, and, hence, one should resort to the new result in Theorem 7 for a frequency-domain stability analysis. Using $G_{yu}(s)$ as in (42) we can construct $G_x(s)$ and $G_y(s)$ as in (39) needed for the analysis. The corresponding Popov-like plot with values $k = \{2, 15\}$ is
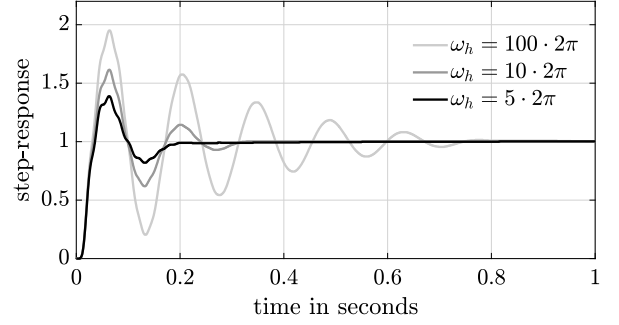

Fig. 7. Measured time-responses of the closed-loop system with $\omega_h \in \{5, 10, 100\} \cdot 2\pi$ rad/s when subject to a step input $r(t) = 1$ for $t \in \mathbb{R}_{\geq 0}$ and $r(t) = 0$ otherwise.

shown in Fig. 6. Clearly, for the value $k = 2$ which corresponds to our preliminary result in [28] it is impossible to find a value for λ such that the conditions in Theorem 7 are satisfied, as part of the corresponding curve lies to the left of the point $(-1, 0)$. On the other hand, for the value $k = 15$ we find that with $\lambda = 10$ the frequency-domain inequality in (40) is satisfied, such that, together with stability of the gain-mode subsystem, all conditions of Theorem 7 are satisfied. Hence, the closed-loop system is ISS. Note that this was only possible to show with our new conditions. The smallest value for which ISS could be shown on the basis of Theorem 7 was found to be $\omega_h = 1.5 \cdot 2\pi$ rad/s. For smaller values of ω_h, satisfaction of the conditions in Theorem 7 is limited by the fact that the gain-mode dynamics become unstable. Note that in the set of LMIs (13) the gain-mode matrix A_2 does not necessarily need to be Hurwitz, thereby indicating room for improvement in the frequency-domain conditions.

Typical step-responses of the closed-loop system for $\omega_h \in \{5, 10, 100\} \cdot 2\pi$ rad/s are shown in Fig. 7, and demonstrate the beneficial effect of reducing ω_h on transient properties such as overshoot and settling times.

6 Conclusions

In this paper, novel frequency-domain conditions for ISS of HIGS-controlled systems have been presented. In contrast to existing conditions, our new condition allows for the existence of a quadratic ISS-Lyapunov function that is strictly positive only within the relevant subregion of the state space, where the dynamics of HIGS are active, as was shown by linking the conditions to a set of LMIs. The conditions provide a substantial advantage over existing results in the sense of significantly reducing conservatism in the analysis for practically relevant scenarios. This was shown on an experimental set-up for which existing frequency-domain tools were not applicable while our new ones were effective. In the example, we illustrated how the derived frequency-domain conditions

can be verified graphically in a manner that is comparable to the classical Popov plot. The conditions derived in this paper may contribute to further development of less conservative, and practically verifiable frequency-domain conditions for nonlinear and hybrid systems in general, and HIGS in particular. Interesting directions for future work include lifting the relative degree two assumption and extending the frequency-domain conditions to multivariable systems.

References

[1] J. Freudenberg, R. Middleton and A. Stefanopoulou. A survey of inherent design limitations, *Proceedings of the American Control Conference*, pp. 2987-3001, 2000.

[2] J.C. Clegg. A nonlinear integrator for servomechanisms (Part II), *Transactions of the AIEE*, vol. 77, pp. 41-42, 1958.

[3] D. Nesic, A.R. Teel, and L. Zaccarian. Stability and performance of SISO control systems with first order reset elements, *IEEE Trans. Autom. Control*, 56, pp. 2567-2582, 2011.

[4] G. Zhao, D. Nesic, Y. Tan, and C. Hua. Overcoming overshoot performance limitations of linear systems with reset control, *Automatica*, 101, pp. 27-35, 2019.

[5] Y. Zheng, Y. Chait, C.V. Hollot, M. Steinbuch, and M. Norg. Experimental demonstration of reset control design, *Control Engineering Practice*, 8, pp. 113-120, 2000.

[6] C. Prieur, I. Queinnec, S. Tarbouriech and L. Zaccarian. Analysis and Synthesis of Reset Control Systems, *Foundations and Trends in Systems and Control*, 6, pp 117-338, 2018.

[7] W. Foster, D. Giesenking and W. Waymayer. A Nonlinear Filter for Independent Gain and Phase (With Applications). *Transactions of ASME Journal of Basic Engineering*, 88, pp. 457-462, 1996.

[8] B. Sharif, A. van der Maas, N. van de Wouw, and W.P.M.H. Heemels. Filtered Split-Path Nonlinear Integrator: A Hybrid Controller for Transient Performance Improvement, *Transactions on Control Systems Technology*, 30(2), pp. 451-463, 2022.

[9] D.A. Deenen, B. Sharif, S.J.A.M. van den Eijnden, H. Nijmeijer, W.P.H.M. Heemels, and M.F. Heertjes. Projection-based integrators for improved motion control: Formalization, well-posedness and stability of hybrid integrator-gain systems, *Automatica*, 133. 2021.

[10] S.J.A.M. van den Eijnden, M. F. Heertjes, W. P. M. H. Heemels and H. Nijmeijer. Hybrid Integrator-Gain Systems: A Remedy for Overshoot Limitations in Linear Control?, in IEEE Control Systems Letters, 4(4), pp. 1042-1047, 2020.

[11] E.D. Sontag, Y. Wang. On characterizations of the input-to-state stability property, *Syst. Control Lett.*, 24, pp. 351-359, 1995.

[12] K. Shi, N. Nikooienejad, I. R. Petersen, and S. O. R. Moheimani. A negative imaginary approach to hybrid integrator-gain system control, 2022, CDC, pp. 1968–1973.

[13] S.J.A.M. van den Eijnden, Y. Knops, and M. F. Heertjes, A hybrid integrator-gain based low-pass filter for nonlinear motion control, *Proc. of the CCTA*, Copenhagen, Denmark, pp. 1108-1113, 2018.

[14] G.A. Leonov, D.V. Ponomarenk, V.B. Smirnova. Frequency-Domain Methods for Nonlinear Analysis: Theory and Applications, World Scientific Series on Nolinear Science Series A, 9, 1996.

[15] H.K. Khalil, Nonlinear Systems. Prentice Hall, Upper Saddle River, New Jersey, 2002.

[16] S.J.L.M. van Loon, K.G.J. Gruntjens, M.F. Heertjes, N. van de Wouw, W.P.M.H. Heemels. Frequency-domain tools for stability analysis of reset control systems. *Automatica*, 82, 101-108, 2017.

[17] O. Beker, C.V. Hollot,Y. Chait, Y. H. Han. Fundamental properties of reset control systems. *Automatica*, 40. pp. 905-915, 2014.

[18] A. A. Dastjerdi, A. Astolfi and S. H. HosseinNia. A Frequency-Domain Stability Method for Reset Systems, 2020 59th IEEE Conf. on Dec. and Control (CDC), South Korea, pp. 5785-5791, 2020.

[19] V.A. Kamenetskiy. Frequency-Domain Stability Conditions for Hybrid Systems. *Automation and Rem. Cont.* 78(12) pp. 2101-2119, 2017.

[20] V.A. Kamenetskiy. Switched Systems, Lur'e Systems, Absolute Stability, Aizerman Problem. *Automation and Rem. Cont.* 80, pp. 1375–1389, 2019.

[21] W. M. Griggs, C. K. King, R. N. Shorten, O. Mason, K. Wulff. Quadratic Lyapunov functions for systems with state-dependent switching. *Linear Algebra and its Applications*, 433(1), pp. 52-63, 2010.

[22] C. K. King, W. Griggs, R. N. Shorten. A Kalman-Yakubovich-Popov-type lemma for systems with certain state-dependent constraints. *Automatica*, 47, pp. 2107-2111, 2011.

[23] R. Shorten, M. Corless, K. Wulff, S. Klinge and R. Middleton. Quadratic Stability and Singular SISO Switching Systems, *IEEE Transactions on Automatic Control*, 54(11), pp. 2714-2718, 2009.

[24] M. Kunze, A. Karimi, and R. Longchamp. Frequency-domain controller design by linear programming guaranteeing quadratic stability. In *Proceedings of the 47th IEEE Conference on Decision and Control*, pp. 345-350, 2008.

[25] M. Arcak, M. Larsen and P. Kokotovic. Circle and Popov criteria as tools for nonlinear feedback design. *Automatica*, 39(4), pp. 643-650, 2003.

[26] W. P. M. H. Heemels and A. Tanwani. Existence and Completeness of Solutions to Extended Projected Dynamical Systems and Sector-Bounded Projection-Based Controllers. *IEEE Control Systems Letters*, 7, pp. 1590-1595, 2023

[27] A. Rantzer. On the Kalman-Yakubovich-Popov lemma. *Systems & Control Letters*, 28(1), pp. 7-10, 1996.

[28] S.J.A.M. van den Eijnden, M.F. Heertjes, W.P.M.H. Heemels and H. Nijmeijer. Frequency-domain tools for stability analysis of hybrid integrator-gain systems. In *Proceeding of the European Control Conference*, pp. 1895-1900, 2021.

[29] S.J.A.M. van den Eijnden, W.P.M.H. Heemels, M.F. Heertjes, and H. Nijmeijer. Stability and performance analysis of hybrid integrator-gain systems: A linear matrix inequality approach. *Nonlinear Analysis: Hybrid Systems*, 45, pp. 101192, 2022.

[30] G.F. Franklin, J.D. Powell, and A. Emami-Naeini, *Feedback control of dynamic systems (5th ed.)*, Prentice Hall, 2005.

[31] S. Skogestad and I. Postlethwaite, Multivariable Feedback Control: Analysis and Design. John Wiley and sons, Ltd. 2005.